ISSN 0354-8724 (hard copy) | ISSN 1820-7138 (online)

Pixel and Object-based Land Cover Mapping and Change Detection from 1986 to 2020 for Hungary Using Histogram-based Gradient Boosting Classification Tree Classifier

András Gudmann[A*], László Mucsi[A]

Received: May 06, 2022 | Revised: July 31, 2022 | Accepted: August 10, 2022
doi: 10.5937/gp26-37720

Abstract

The large-scale pixel-based land use/land cover classification is a challenging task, which depends on many circumstances. This study aims to create LULC maps with the nomenclature of Coordination of Information on the Environment (CORINE) Land Cover (CLC) for years when the CLC databases are not available. Furthermore, testing the predicted maps for land use changes in the last 30 years in Hungary. Histogram-based gradient boosting classification tree (HGBCT) classifier was tested at classification. According to the results, the classifier, with the use of texture variance and landscape metrics is capable to generate accurate predicted maps, and the comparison of the predicted maps provides a detailed image of the land use changes.

Keywords: land use; land cover; image classification; change detection; gradient boosting

Introduction

Land use and land cover (LULC) changes can alter the ecosystem and its services, and they can indicate socio-economic changes that have occurred in a particular area (Wulder et al., 2018). By analyzing the LULC changes in detail, we can estimate their complex effects on the environment (impact on landscape structure, biodiversity) and agricultural complexes. With the acceleration of LULC changes that occurred with urban expansion, economic growth, and explicitly/implicitly increasing human needs, the monitoring of LULC changes became a key tool that could be used in work associated with environmental protection and sustainable development. LULC maps are often used as base data in environmental studies conducted in fields such as agriculture (Bezdan et al., 2019), hydrology (Tobak et al., 2019), ecology (Csikós & Szilassi, 2021), urbanization (Steurer & Bayr, 2020), and change detection (Szilassi, 2017). LULC mapping is a widely discussed topic in the field of remote sensing because remote sensing can provide tools, and reliable and extensive data with a high temporal and spatial resolution for LULC mapping (Townshend et al., 1991). It is a challenging classification task, because land use and its categories (nomenclature) depend on the socio-economic environment, thus each country or region will have its own set of land use classes (Choudhury & Jansen, 1999). Thus, the number of land use classes has become large and interclass separability small, which makes training data unbalanced and difficult to classify. Moreover, in most cases, the efficiencies of the spectral values obtained from satellite images are small. Thus, new variables have to

[A] Department of Geoinformatics, Physical and Environmental Geography, University of Szeged, Egyetem utca 2, 6722 Szeged, Hungary; mucsi@geo.u-szeged.hu, gudmandras@geo.u-szeged.hu
[*] Corresponding author: András Gudmann, e-mail: gudmandras@geo.u-szeged.hu

be incorporated into land use classification, which is computationally challenging.

The dataset dimensions (size and number of variables) greatly depend on the scale of mapping and the amount of data used. In large-scale land use mapping, we need to consider the spectral differences among the satellite images and the exponential growth of the dataset as new variables are added, which causes the modeling and prediction times to increase. Therefore, the selection of new data required for land use classification through the application of different sensors in combination (Zhou et al., 2018), use of multitemporal images (Bui & Mucsi, 2021), or extraction of new features (indices, textures, and metrics) from the original image is important (Gudmann et al., 2020; Zhou et al., 2018). In land use change mapping, the use of different sensor data or multitemporal images is not possible in most cases because of the limitations of old datasets. Thus, the only option available is to extract new features, such as spectral indices, texture data, and segmentation from the original satellite images.

In this study, large-scale LULC maps were created on four dates between 1986 and 2020 based on Landsat images, their derivates, and CLC databases. Using these maps, pixel-based change analyses were performed to estimate a detailed picture of the environmental changes that had occurred. Two research questions were tested: first, can we generate LULC maps with CLC nomenclature, accurate enough to use them as a base for a pixel-scale change analysis? Second, if the pixel-scale change analysis is performed based on the generated maps, would the results provide more details than the CLC change layers?

To answer these questions, first, with the use of a histogram-based gradient boosting classification tree, LULC maps were generated. Second, the improvement in land use classification was estimated using pixel-based comparison. Furthermore, pixel-based change detection was performed using the classified maps and the results were compared with the CLC datasets.

Data and methods

Study area

The study area selected was the entire territory of Hungary, located in the Carpathian Basin (Figure 1), with an area of 93 023 km^2. Most of the land area of this east-central European country is occupied by lowlands (more than 80% of the land area is at an elevation between 75 and 200 m above sea level) and only 0.6% of its land area is at an elevation more than 500 m above sea level. The soil in most areas of the country has high organic content, which favors agriculture (Mezősi, 2017). Most of the land area of the country (78.7%) is productive because of its specific soil type and favorable climate, and more than half of the land area (57.1%) is used for agriculture (Hungarian Central Statistical Office, 2020). The agricultural land has a one-sided structure dominated by small holdings (<5 ha in size), which account for more than 80% of the agricultural holdings in the area (European Commission - DG Agriculture and Rural Development, 2020). Most of the landscape of the country

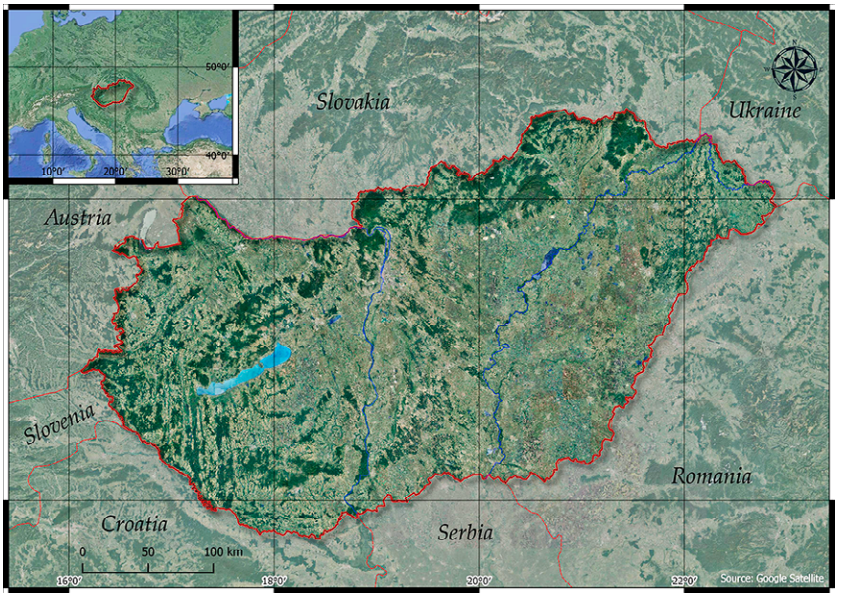

Figure 1. Study area: Hungary in East-Central Europe

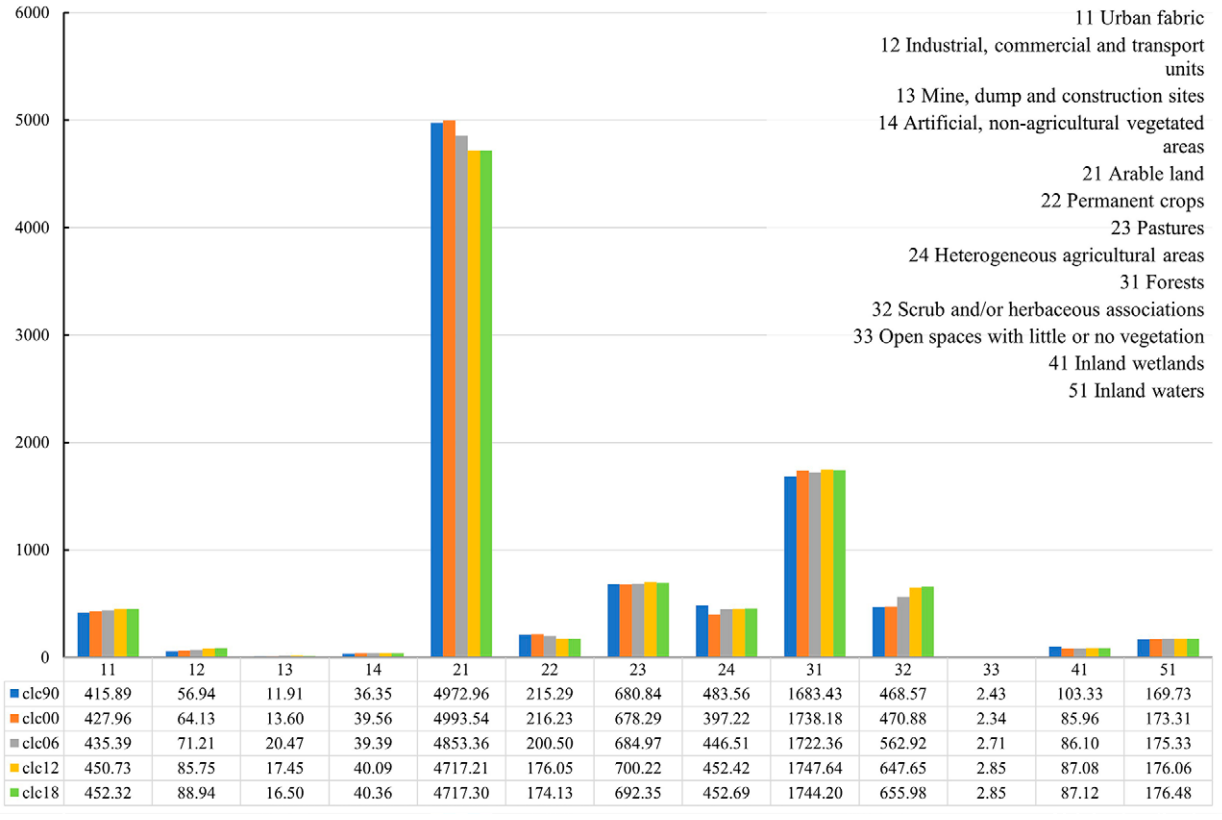

	11	12	13	14	21	22	23	24	31	32	33	41	51
clc90	415.89	56.94	11.91	36.35	4972.96	215.29	680.84	483.56	1683.43	468.57	2.43	103.33	169.73
clc00	427.96	64.13	13.60	39.56	4993.54	216.23	678.29	397.22	1738.18	470.88	2.34	85.96	173.31
clc06	435.39	71.21	20.47	39.39	4853.36	200.50	684.97	446.51	1722.36	562.92	2.71	86.10	175.33
clc12	450.73	85.75	17.45	40.09	4717.21	176.05	700.22	452.42	1747.64	647.65	2.85	87.08	176.06
clc18	452.32	88.94	16.50	40.36	4717.30	174.13	692.35	452.69	1744.20	655.98	2.85	87.12	176.48

Figure 2. Distribution of CLC categories in Hungary in thousand hectares

is fragmented, with low patch sizes, because of its agricultural land structure. According to the CLC databases (Buttner & Kosztra, 2017), more than half of the area of Hungary was covered by arable lands (Figure 2). Besides, the main land cover categories are the forests (~18%), pastures (7%), scrub and/or herbaceous associations (~5-7%), heterogeneous agricultural area (~5%), and urban fabric (~4%).

Data

The reference data of our study was the CORINE Land Cover datasets. These databases were created using a 1:100 000 scale, a minimum mapping unit (MMU) of 25 ha, and a minimum width of 100 m for the linear elements (Mari & Mattányi, 2002). The nomenclature of CLC data is hierarchically structured, with three levels: 5 classes at level 1, 15 classes at level 2, and 44 classes at level 3. Thanks to the detailed nomenclature, spatial (CLC90: 27 countries; CLC18: 39 countries) and temporal coverage (from 1990, five times), and thematic accuracy (>85%), the CLC database is the basis of various research activities. To provide further support to these studies, change layers were created and the changes exceeding 5 ha were mapped. Even with a small MMU, the change layers could not display most of the changes that had occurred at the parcel level because the average size of those changes was below 5 ha (Volker et al., 1998) (Figure 3). In this study, the CLC datasets CLC90, CLC00, CLC06, CLC12, and CLC18 were used as reference datasets in land use classification. The CLC change layer was used as the reference in the change analysis. The CLC databases were downloaded from the website of the Copernicus Land Monitoring Service at https://land.copernicus.eu/pan-european/corine-land-cover.

For the study, Landsat satellite images were selected, because of the similarity of their spatial and spectral resolutions. The data acquisition devices provided in the satellites are designed to take images, comparable to one another, to facilitate data continuity and time-series analyses (Wulder et al., 2016). The Landsat images have a medium spatial resolution (30, 60, and 80 m), multispectral resolution (4–11 bands), and a 16-day temporal resolution (U.S.Geological Survey, 2012). The image archive has global coverage and is freely available to any user (Wulder et al., 2019). Ten Landsat images were required to cover the study area, with low cloud cover and low temporal differences, which reduced the spectral image differences. According to these conditions, 4 dates were selected, with a large time interval: 1986, 2003, 2015, and 2020. The atmospherically corrected Landsat images with surface reflectance were ordered and downloaded from the USGS Earth Resources Observation and Science Center Science Processing Architecture system on-demand interface, available at https://espa.cr.usgs.gov/.

Figure 3. Parcel-level changes in an agricultural area, near Nagyszénás village. Based on the CLC polygons (yellow lines), no change occurred

Derivatives describing the pixel neighborhood were calculated using the satellite images to provide the information required by the classification model. Two types of derivatives were generated: variance texture information with different kernel sizes (7x7, 17x17) and landscape metrics (the mean patch size, the total edge, mean shape index, and mean fractal dimension).

Methods

Data processing was conducted using ERDAS Imagine 2020, QGIS 3.4.4, and ArcMap 10.3 software, and the classifications were performed in a Python 3.7 programming environment (Figure 5). To reduce the loss of accuracy due to spectral differences, the Landsat images (10 images per date) were mosaicked along the same path (according to the WRS-2 catalogue, 4 paths: 189, 188, 187, 186). The images along the paths (i.e., zones) were put together using manually drawn seamline polygons (Figure 4). These zones were the base areas of the classification. The created mosaics were used for texture and landscape metric calculations. For each band, texture images were generated using variance metric and two different kernel sizes: 7 × 7 (210 × 210 m) and 17 × 17 (510 × 510 m) with ERDAS built-in texture calculator. For the landscape metrics, each satellite mosaics were segmented at a minimal size of 25 ha, and

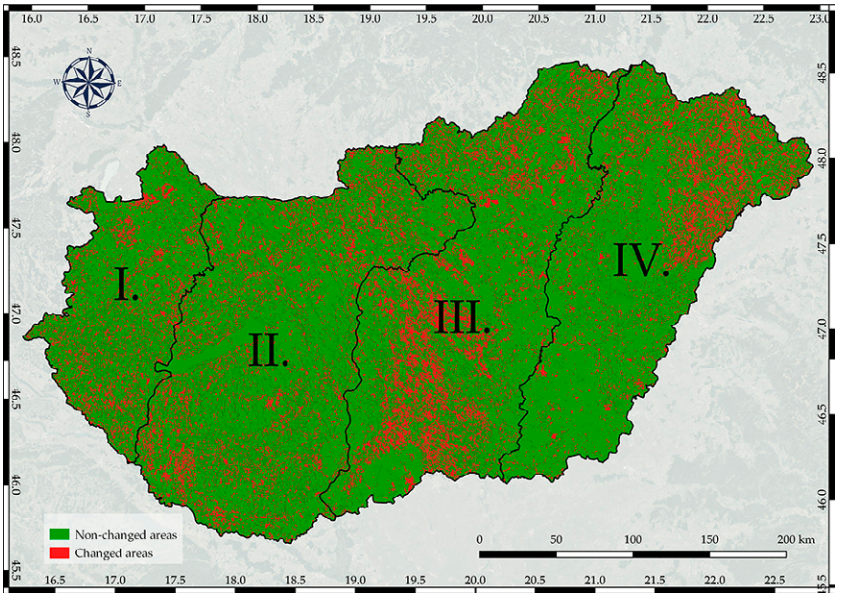

Figure 4. The four zone and the changed/non-changed areas

the metrics were calculated using the V-Late 2 ArcGIS tool (Comber et al., 2000). The six spectral bands (B, G, R, NIR, SWIR 1, and SWIR 2), texture bands, and landscape metrics of the satellite images were stacked together to generate images with 22 layers.

The CLC datasets were processed to identify the areas that have not changed over the last 30 years, in order to reduce the uncertainty (<=15%) of the points from the CLC reference data. To this end, all CLC datasets were intersected with one another, and the polygons with the same CLC code were selected. These unchanged areas are 81.1% of the whole area, thus they are capable to represent the whole study area (Figure 4). The selected polygons were exported and were split into four parts like the stacked images (Figure 4). For each part, training and validation point sets were generated inside the selected polygons. The validation points were generated around the polygons' centroids, while the training points are randomly inside the polygons. The number of training points is less than 2% of the whole area.

From the training and validation points, 20 points per class per set were randomly selected and visually checked based on medium- and high-resolution satellite images and high-resolution aerial images at all dates. The result of the points verification showed all CLC categories reached the CLC base thematic accuracy, thanks to the use of the non-changed areas. The mean accuracy of the training points, on one date is greater than 93% (lowest, 2020: 93.7%, highest, 1986: 95.18%), while the validation points' mean accuracy is greater than 97% (lowest, 2020: 97.59%, highest, 1986: 98.89%).

Using the point sets created the values of each band of the stacked images and the codes of the CLC databases were extracted and exported to the csv files. For each date and each part of the study area, one training and one validation file was created. These csv files were used in the HGBCT classification python script. The HGBCT is a type of gradient boosting machine (GBM) (Friedman, 2001). It is an ensemble machine learning method, which can use different base learners (decision trees and neural networks) for classification or regression tasks. The GBM builds the model in a forward stage-wise mode, which allows for the optimization of an arbitrary differentiable loss function (Friedman, 2002). The HGBCT displays high accuracy when used with big datasets, is robust in handling missing values and unbalanced datasets, and has a low model building and prediction times. The classification method was implemented using the grid-search parameter estimation (or hypertuning) method to estimate the best parameters that can be used in model building. For each zone, different models were built.

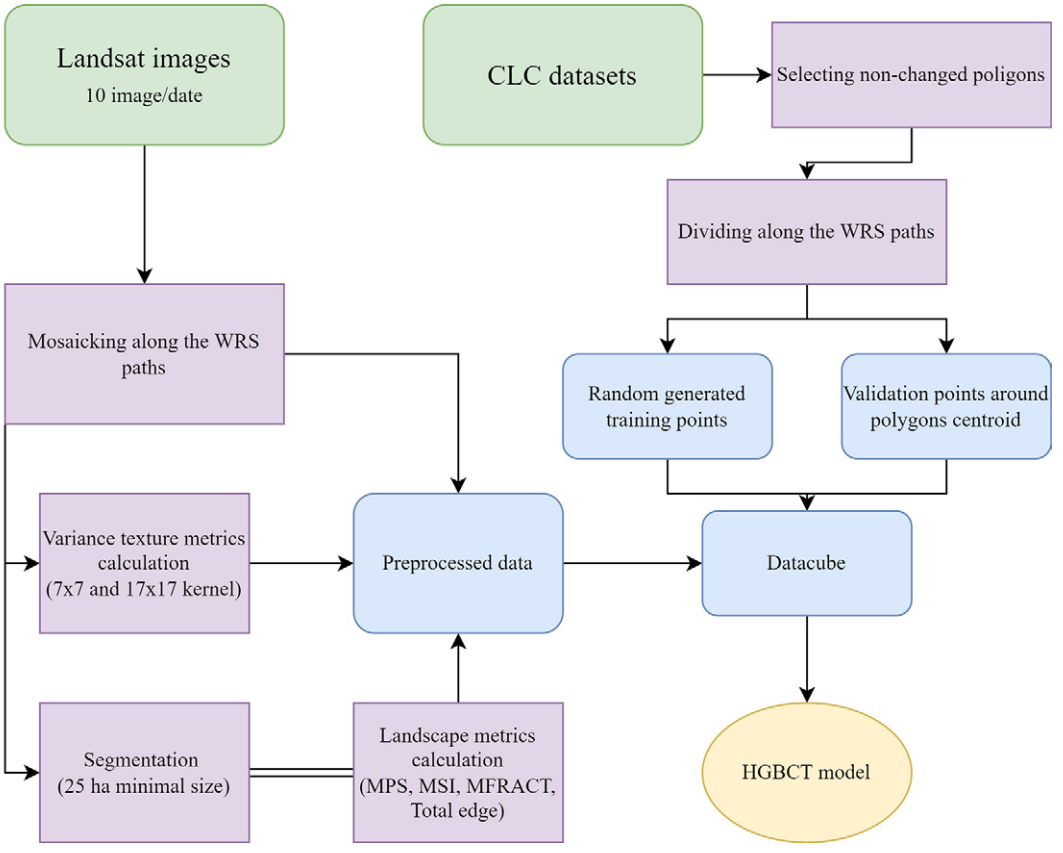

Figure 5. Data processing workflow

Results

Modeling and mapping

During the modeling and mapping stage, the HGBCT classification method was applied and tested. The test model building, and predictions were made using the training and validation sets of the datasets collected on different date's datasets. As a result of hypertuning, the following hyperparameters of HGBCT enabled its highest accuracy: maximum number of iterations: 1200 with early stopping applied, learning rate: 0.01, maximum depth of each tree: 20; minimum number of samples per leaf: 75, and maximum number of leaves allowed for each tree: 256. During model building, different values were observed, like overall accuracy (OVRA), kappa, and logarithmic loss. The overall accuracies of the gradient boosting models were between 83.35% (2015: Zone II.) – 92.63% (1986: Zone I.). The User's accuracies (UAs) of the classifier were varied between 61.79% and 100%, 60.30% and 100%, 60.61% and 100%, and 62.30% and 100% in 1986, 2003, 2015, and 2020, respectively. More than half the classes (15 of 27) had UAs exceeding 90% and none of the classes had UAs below 60%. Only one class, the originally mixed, 242–Complex cultivation patterns, had a UA near 60%. The PAs were in the 56.49%–99.69%, 56.34%–99.85%, 53.86%–100%, and 51.19%–100% ranges in 1986, 2003, 2015, and 2020, respectively. Most of the Producer's accuracies (PAs) had high accuracies as the UAs, with 17 of the 27 classes recording accuracies higher than 90%. Only the "Non-irrigated arable land" class has a low accuracy (51.19%–56.49%), it deserves to be highlighted because it has the largest extent in the study area thus, it has a huge impact on change mapping. The average overall accuracy of the models per date was between a small range of 85.99% – 87.33%. The kappa values of the models varied between 0.83 and 0.92, while the log loss values were be-

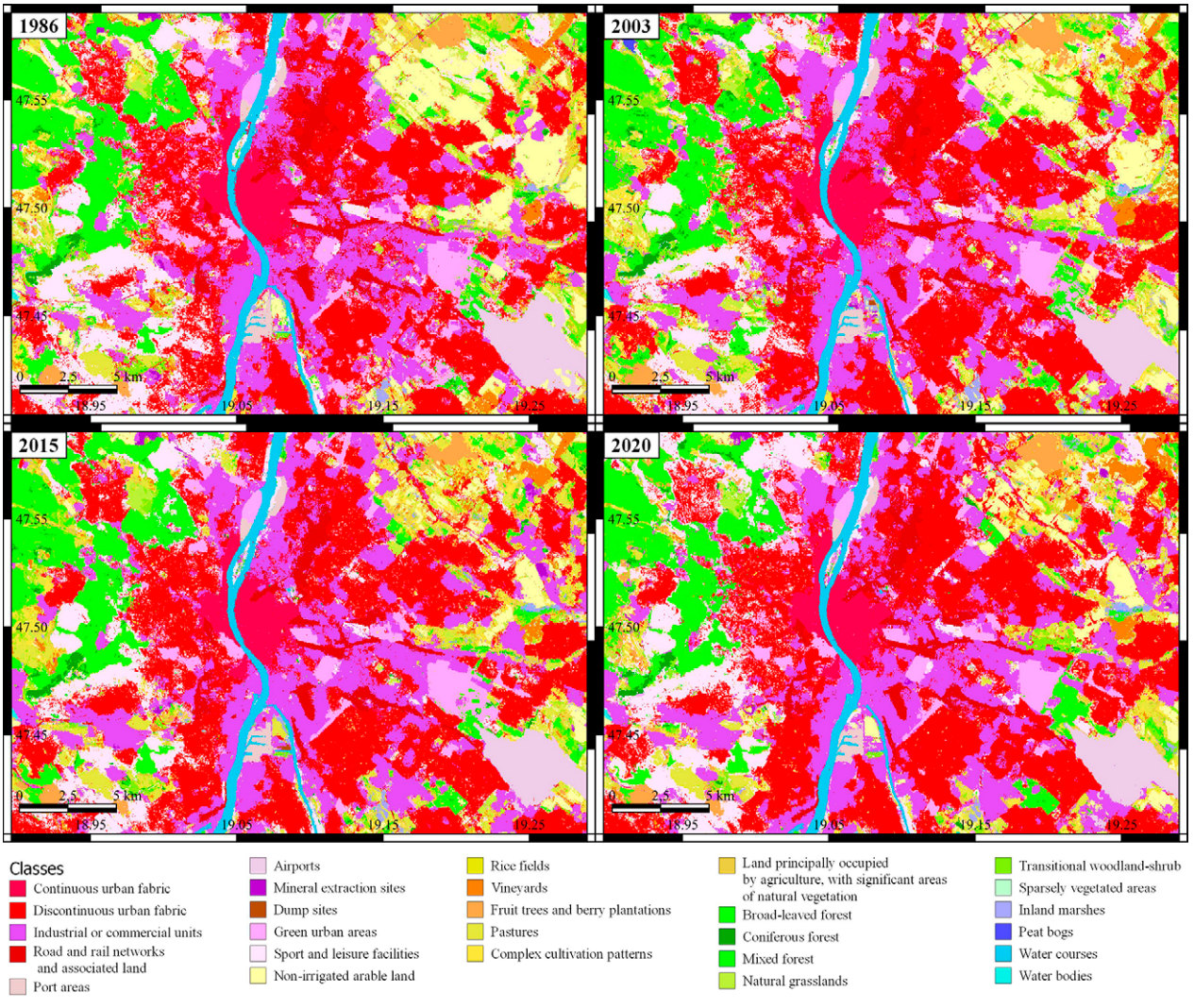

Figure 6. Classified maps of Budapest, the capital of Hungary, at different date

tween 0.26 and 0.56. The appearances of the classified maps are compact and smooth (Figure 6). The different values of the model building indicate that all models were suitable for accurate land use classification.

Land use change analysis

Land use change mapping was performed using a pixel-based comparison of the predicted maps of the HG-BCT models. The maps were compared, and three land use change maps were generated (1986–2003, 2003–2015, and 2015–2020). Using these maps, land use change matrixes were created and the changes were categorized into six groups based on the work of Feranec (Feranec et al., 2010). The six groups are urbanization, agricultural intensification, agricultural extensification, afforestation, deforestation, and water body construction. This categorization includes permanent and temporary land use changes, thereby enabling short- and long-time series analyses. However, the magnitude of the detected changes could be large. The first period of the changes is between 1986-2003. During this period, the socialist system has replaced, and the economy drastically changed. The most spectacular sign of these changes was the fragmentation of agricultural land, due to compensations and privatization. According to the CLC change layer, the magnitude of the mean yearly area transformation was 0.497% (1990–2000) (Table 1).

The biggest mean yearly changes were afforestation and deforestation, where the afforestation had a bigger magnitude, thus the proportion of the forest increased. Besides, the intensification and extensification of agriculture had a similar value, with notable magnitude. According to the comparison of the predicted maps, the magnitude of changes was apparently larger than what the CLC change layer displayed (Table 2).

Unlike, the CLC change layers, the biggest change was in agriculture (intensification and extensification), where intensification had a clearly bigger role. Like at CLC change layers, the afforestation and deforestation had a big magnitude, but the difference between the two opposite processes was much bigger. Furthermore, the urbanization process was clearly more serious, than the values of the CLC. The second period was between 2003-2015. During this period, the driving force of the changes was Hungary's accession to the EU, the responsibilities associated with it, and the significant subsidies for different projects. Due to this, the image of the production of Hungary had changed, which brought with it a change in land use/land cover. In the middle of the period, because of the economic crisis, the changes slowed down. However, after the recovery, large-scale industrial and public investment began. In this period, financially supported afforestation began. Despite this, the CLC change layers show only a slight change in the magnitude of the afforestation and a strong decrease in deforestation, while the agricultural changes remained significant, and accelerated. Besides, the rate of urbanization was slightly increased, and the water body construction was decreased. According to the predicted maps, the magnitude of the agriculture (intensification and exten-

Table 1. Mean yearly categorized land use changes, based on CLC change maps

Date	1990–2000	2006–2012	2012–2018
Urbanization	0.0112%	0.0176%	0.0151%
Intensification of agriculture	0.0804%	0.1305%	0.042%
Extensification of agriculture	0.0728%	0.0865%	0.0215%
Afforestation	0.1815%	0.1831%	0.0938%
Deforestation	0.1465%	0.0948%	0.0848%
Water body construction	0.0052%	0.0035%	0.0023%
Total change	0.497%	0.516%	0.259%

Table 2. Mean yearly categorized land use changes, based on the predicted change maps

Date	1986–2003	2003–2015	2015–2020
Urbanization	0.184%	0.323%	0.71%
Intensification of agriculture	0.632%	0.866%	2.162%
Extensification of agriculture	0.428%	0.609%	1.424%
Afforestation	0.345%	0.538%	1.264%
Deforestation	0.178%	0.247%	0.726%
Water body construction	0.035%	0.061%	0.128 %
Total change	1.802%	2.643%	6.414%

sification) changes was increased, compared to the previous period. Furthermore, the rate of afforestation had increased, and thus twice as much as deforestation. In addition, the rate of urbanization increased by 0.134%/year. These results are in line with the economic measures introduced. The last period was only 5 years, between 2015-2020. During these 5 years, the large public investments continued and began the growth of the housing sector. Furthermore, the financially supported afforestation continued with greater magnitude. These events are well discernible from the predicted map values. In this short time range, the urbanization, the afforestation, the deforestation, and the water body construction processes were accelerated, and thus their values were doubled. While, agricultural changes remained the causes of the biggest impact, with a significant increase. On contrary to that, the CLC change layers show slowing changes. The rate of afforestation was halved, while the rate of the intensification of agriculture showed a bigger decrease. Besides, the extensification of agriculture decreased substantially. In the other categories, the magnitude of the slowing was small. In conclusion, at the CORINE Land Cover change layers, the magnitude of the area transformation can be between 0.497%/year (1990–2000), 0.516%/year (2006-2012), and 0.259%/year (2012–2018) of the total area, with a decreasing rate. The main change flows are afforestation and deforestation and the transition of agricultural lands. Considering deforestation, afforestation would have the largest impact on an area. The transitions of the agricultural lands had a big impact in the first and second periods, while in the third period it had a small impact. Urbanization had a moderate impact on the changes in every period. The water body construction had the smallest volume, with a continuous decrease. While, according to the results of pixel-based analysis of the predicted maps, the magnitude of changes was apparently larger than what the CLC change layer displayed (1.802%/year – 6.414%/year). The urbanization was between 0.184%/year and 0.71%/year, which is significantly bigger, than the CLC values. The transformation of the agricultural lands dominates agricultural intensification, which is approximately one and half times the magnitude of extensification. These values are more than hundred times bigger than the values of the CLC change layers. The afforestation is almost twice deforestation, and thus, the size of the forests is on the increase, in the same way as the CLC layers, but the magnitude of these changes is bigger. The rate of water body construction is low and is the smallest of all, but with continuous increase. Apart from these change categories, some uncategorized changes also exist, but their magnitudes are low. Thus, they were not included in this study. The magnitude of the changes detected is large, because of the pixel level scale used. Using pixel-based categorization, permanent and temporary changes can be predicted. Most of these changes are temporary, and they appear in turns in a particular area, such as agricultural intensification and extensification or afforestation and deforestation. Further information can be obtained by visually analyzing the maps. The visual analysis of the maps helps determine the localization and the level of permanency of the changes. According to the analysis results, most changes were not permanent and were due to the behavior of the economy (cutting and replanting artificial forests, setting aside arable land, and crop rotation). Urbanization and afforestation are two permanent changes. Urbanization is a one-way change (as mentioned earlier) and thus, it is permanent. It appears mainly in and around the main cities of Hungary. Afforestation is not a permanent transformation, but if afforestation is higher than deforestation in magnitude, a permanent change has occurred. According to the results of the visual analysis, permanent afforestation is concentrated mainly in agricultural areas in the Great Hungarian and Little Hungarian Plains. These permanent changes reduce the size of agricultural land, and explains the rate of agricultural intensification. Overall, the land use change maps created provide detailed information about land use transformations in Hungary that have occurred over the last 30 years, which were dominated by agricultural intensification, afforestation, and gradual and slow urbanization.

Discussion

This study aimed to test a possible classification method, to create large-scale LULC maps on 4 dates. Furthermore, we tested these predicted maps in a large-scale, pixel-based change analysis. In the presented method, we used the HGBCT classifier to create maps, based on Landsat imagery with landscape metrics and texture data. By considering the predicted map, land use change analysis was performed, which matched the CLC change layers. The land use change mapping method presented meets the preliminary expectations.

Many studies have focused on land use/land cover classification in different scenarios. McCarty et al. compared three different algorithms (random forest, SVM, and light GBM) for large-scale land use mapping (McCarty et al., 2020). In their classification sce-

nario, seven classes were targeted, and the light GBM had the highest overall accuracy (65.3%) and random forest had the lowest overall efficiency (59.4%). Malinowski et al. created an automated CLC mapping method using the random forest classifier and a modified nomenclature, which had only 13 classes (Malinowski et al., 2020). Using this method, they could successfully create land use maps for the whole area of Europe, with an overall accuracy of 86.1% at the continental level. A very similar study to our research wasmade by Marco Calder 'on-Loor et al. (Calderón-Loor et al., 2021). They made a land cover/use mapping and change analysis for Australia from 1985 to 2015, with 5-year steps. They used Google Earth Engine to process a high amount of Landsat images (>200 000) to create composite images. They classified the preprocessed images into six land cover classes with a random forest model. With this high number of images and a low number of classes they reach a very high accuracy (<93%) and made a satisfactory change analysis. A global land cover map made by Karra et al. (Karra et al., 2021). They created land use maps with the use of Sentinel-2 images and hand-labeled reference datasets, which contains 10 classes. For classification purposes, they utilized a UNet neural network for image segmentation and to classify the segments. The results showed, the usefulness of the UNet network at land cover classification, where every class reached >85% accuracy. These surveys are showing very good results at large-scale classification, but the applied nomenclatures were mainly limited to land cover classes.

The results of our presented method show a significant progress. In our classification scenarios, we used more than 20 classes with low separability values and big monotemporal datasets. Despite the use of this difficult scenario, the HGBCT classifier achieved satisfactory results (83.35%–92.63%). The other model-performance metrics, such as log loss and kappa, show corresponding results. Furthermore, the UAs and PAs of the models were high, only the class 211–Non-irrigated arable land, which has the largest extent, obtains a low PA. This low PA can occur for reasons such as training point randomness, class mixture caused by the CLC's MMU, and combination of the pixel-based mapping unit and an accurate model. As most of these reasons cannot be eliminated, the problem could occur in every setting of the method. According to these results, our predicted map was suitable for change mapping. Land use change mapping is difficult to evaluate because the relevant databases would have been created using different methodologies (nomenclatures, MMUs, and reference data). In this study, land use change maps were created at the pixel level (900 m^2) using the CLC nomenclature. The CLC change layers and the predicted change maps were comparable. However, the two datasets have different time-range, which slightly distorts the comparison. Besides, the MMUs of the two datasets were different (CLC change layers had 5-ha changes). Thus, the predicted maps had more details and larger values in certain categories than the CLC change layers, and their range of statistics was much larger. This difference could be attributed to the magnitudes of the changes, which were much bigger in the predicted maps (1.802%/year – 6.414%/year) than in the CLC change layers (0.259%/year – 0.516%/year). The MMU had a large impact on the analysis because the majority of the changes occurred in small and separate areas; thus, they are not shown in CLC change layers and may not be permanent, which is true especially in agriculture in which are many small parcels. These temporary, likely parcel-level, agricultural changes are responsible for approximately half of the changes. Overall, the predicted maps contain both permanent and temporary changes and thus provide a detailed picture of the land use changes in the country. Thus, the maps can be used in detailed surveys.

Conclusion

The large-scale land use mapping contains several difficulties: available data sources, size of the data, nomenclature, etc. Our study demonstrated a possible solution, where we created LULC maps with the combined use of spectral bands, and variance texture data landscape metrics. According to the study findings, with the aforementioned information, when used as input layers in classification, we predicted maps with high accuracy (83.35%–92.63%). Land use change maps were created by comparing the land use maps at pixel-level, that were created. The created maps contain details of permanent and temporary changes, and are, therefore, adequate for the various types of analyses. The results revealed that more studies using carefully chosen training points are required to examine the impact of training point selection, and the importance of the MMU of the reference data. Moreover, using different change categorizations, detailed change flows would become observable.

Acknowledgments

This research was supported by National Scientific Research Funds (Hungary) in support of the ongoing research: 'Time series analysis of land cover dynamics using medium- and high-resolution satellite images' (NKFIH 124648K) at the Department of Geoinformatics, Physical and Environmental Geography of the University of Szeged. This research was supported by the Ministry of Innovation and Technology of Hungary from the National Research, Development and Innovation Fund, financed under the TKP2021-NVA-09 project number.

References

Bezdan, A., Vranešević, M., Blagojević, B., Pejić, B., Bezdan, J., Milić, D., Tica, N., & Zekić, V. (2019). Agricultural Drought Risk Assessment in Vojvodina. In Z. Ladányi & V. Blanka (Eds.), *Monitoring, risks and management of drought and inland excess water in South Hungary and Vojvodina* (pp. 226–239). University of Szeged Department of Physical Geography and Geoinformatics Projekt.

Bui, D. H., & Mucsi, L. (2021). From Land Cover Map to Land Use Map: A Combined Pixel-Based and Object-Based Approach Using Multi-Temporal Landsat Data, a Random Forest Classifier, and Decision Rules. *Remote Sensing*, 13(9), 1700. https://doi.org/10.3390/rs13091700

Buttner, G., & Kosztra, B. (2017). CLC2018 *Technical Guidelines*.

Calderón-Loor, M., Hadjikakou, M., & Bryan, B. A. (2021). High-resolution wall-to-wall land-cover mapping and land change assessment for Australia from 1985 to 2015. *Remote Sensing of Environment*, 252, 112148. https://doi.org/10.1016/j.rse.2020.112148

Choudhury, K., & Jansen, L. (1999). T*erminology for Integrated Resources Planning and Management*.

Comber, A. J., Birnie, R. V., & Hodgson, M. (2000). Using landscape metrics to model land cover change. In T. Clare & D. Howard (Eds.), *9th annual conference of the international-association-for-landscape ecology* (pp. 143–161). Proceedings of the International Association of Landscape Ecology (UK) Conference: Quantitative approaches to Landscape Ecology.

Csikós, N., & Szilassi, P. (2021). Modelling the Impacts of Habitat Changes on the Population Density of Eurasian Skylark (Alauda arvensis) Based on Its Landscape Preferences. *Land*, 10(3), 306. https://doi.org/10.3390/land10030306

European Commission - DG Agriculture and Rural Development, F. E. U. (2020). *Statistical Factsheet - Hungary*.

Feranec, J., Jaffrain, G., Soukup, T., & Hazeu, G. (2010). Determining changes and flows in European landscapes 1990–2000 using CORINE land cover data. *Applied Geography*, 30(1), 19–35. https://doi.org/10.1016/j.apgeog.2009.07.003

Friedman, J. (2001). Greedy Function Approximation: A Gradient Boosting Machine. *Annals of Statistics*, 29, 1189–1232. https://doi.org/10.2307/2699986

Friedman, J. (2002). Stochastic Gradient Boosting. *Computational Statistics & Data Analysis*, 38, 367–378. https://doi.org/10.1016/S0167-9473(01)00065-2

Gudmann, A., Csikós, N., Szilassi, P., & Mucsi, L. (2020). Improvement in Satellite Image-Based Land Cover Classification with Landscape Metrics. *Remote Sensing*, 12(21), 3580. https://doi.org/10.3390/rs12213580

Hungarian Central Statistical Office. (2020). *Statistical Pocketbook of Hungary, 2019* (V. G. Dr. Bódiné (ed.)). Hungarian Central Statistical Office.

Karra, K., Kontgis, C., Statman-Weil, Z., Mazzariello, J. C., Mathis, M., & Brumby, S. P. (2021). GLOBAL LAND USE/LAND COVER WITH SENTINEL 2 AND DEEP LEARNING. *International Geoscience and Remote Sensing Symposium (IGARSS), 2021-July*, 4704–4707. https://doi.org/10.1109/IGARSS47720.2021.9553499

Malinowski, R., Lewiński, S., Rybicki, M., Gromny, E., Jenerowicz, M., Krupiński, M., Nowakowski, A., Wojtkowski, C., Krupiński, M., Krätzschmar, E., & Schauer, P. (2020). Automated Production of a Land Cover/Use Map of Europe Based on Sentinel-2 Imagery. *Remote Sensing*, 12(21), 3523. https://doi.org/10.3390/rs12213523

Mari, L., & Mattányi, Z. (2002). Egységes európai felszínborítási adatbázis a CORINE Land Cover program (A uniform european land cover database the CORINE Land Cover program). *Földrajzi Közlemények*, 76 (50), 31–38.

McCarty, D. A., Kim, H. W., & Lee, H. K. (2020). Evaluation of Light Gradient Boosted Machine Learning Technique in Large Scale Land Use and Land Cover Classification. *Environments*, 7(10), 84. https://doi.org/10.3390/environments7100084

Mezősi, G. (2017). *The Physical Geography of Hungary*. Springer International Publishing.

Steurer, M., & Bayr, C. (2020). Measuring urban sprawl using land use data. *Land Use Policy*, 97, 104799. https://doi.org/10.1016/j.landusepol.2020.104799

Szilassi, P. (2017). Land cover variability and the changes of land cover pattern in landscape units of Hungary. *Journal of Landscape Ecology*, 15, 131–138.

Tobak, Z., Leeuwen van, B., Kovács, F., & Szatmári, J. (2019). High precision mapping and monitoring of inland excess water inundations. In Z. Ladányi & V. Blanka (Eds.), *Monitoring, risks and management of drought and inland excess water in South Hungary and Vojvodina* (pp. 13–23). University of Szeged Department of Physical Geography and Geoinformatics.

Townshend, J., Justice, C., Li, W., Gurney, C., & McManus, J. (1991). Global land cover classification by remote sensing: present capabilities and future possibilities. *Remote Sensing of Environment*, 35(2), 243–255. https://doi.org/10.1016/0034-4257(91)90016-Y

U.S.Geological Survey. (2012). Landsat: A global land-imaging mission. In *Fact Sheet*. https://doi.org/10.3133/fs20123072

Volker, A., Mezősi, G., & Mucsi, L. (1998). Die Pußta. Historisch-geographische und geoökologische Aspekte eines schulgeographischen und touristischen Leitbildes von Ungarn in Ungarn. In *Natur - Raum - Geselschaft* (pp. 175-217.). Johann Wolfgang Goethe-Universität Frankfurt.

Wulder, M. A., Coops, N. C., Roy, D. P., White, J. C., & Hermosilla, T. (2018). Land cover 2.0. *International Journal of Remote Sensing*, 39(12), 4254–4284. https://doi.org/10.1080/01431161.2018.1452075

Wulder, M. A., Loveland, T. R., Roy, D. P., Crawford, C. J., Masek, J. G., Woodcock, C. E., Allen, R. G., Anderson, M. C., Belward, A. S., Cohen, W. B., Dwyer, J., Erb, A., Gao, F., Griffiths, P., Helder, D., Hermosilla, T., Hipple, J. D., Hostert, P., Hughes, M. J., … Zhu, Z. (2019). Current status of Landsat program, science, and applications. *Remote Sensing of Environment*, 225, 127–147. https://doi.org/10.1016/j.rse.2019.02.015

Wulder, M. A., White, J. C., Loveland, T. R., Woodcock, C. E., Belward, A. S., Cohen, W. B., Fosnight, E. A., Shaw, J., Masek, J. G., & Roy, D. P. (2016). The global Landsat archive: Status, consolidation, and direction. *Remote Sensing of Environment*, 185, 271–283. https://doi.org/10.1016/j.rse.2015.11.032

Zhou, T., Li, Z., & Pan, J. (2018). Multi-Feature Classification of Multi-Sensor Satellite Imagery Based on Dual-Polarimetric Sentinel-1A, Landsat-8 OLI, and Hyperion Images for Urban Land-Cover Classification. *Sensors*, 18(2), 373. https://doi.org/10.3390/s18020373